VARIATION OF RESPONSE SPECTRUM WITH TECTONIC ENVIRONMENT AND FOCAL DEPTH

Grant T. Lindley* and Ralph J. Archuleta#

*Institute for Crustal Studies
University of California
Santa Barbara CA 93106-1100

#Department of Geological Sciences and
Institute for Crustal Studies
University of California
Santa Barbara CA 93106-1100

ABSTRACT

The variation of response spectral shapes is examined for the 1980 Mammoth Lakes, 1983 Coalinga, and 1992 Southern California earthquake sequences. Significant variations of the response spectra are found between earthquakes of the Southern California earthquake sequence and earthquakes of the Mammoth Lakes and Coalinga sequences. These variations do not correspond simply to variations with tectonic environment. Variation of response spectral shape with focal depth is found for microearthquakes, but not for large, potentially damaging earthquakes (M >6). Response spectral shapes vary with magnitude and the variation is significant when the difference in magnitude is approximately 2 or larger.

INTRODUCTION

The 1991 Unified Building Code (UBC) gives normalized response spectra to be used in the design of structures. The shapes of these spectra vary depending on geotechnical site parameters but not on earthquake source characteristics. Source characteristics are taken into account primarily by the peak ground acceleration. Various studies have found the peak ground acceleration of earthquakes to vary with focal depth and/or tectonic environment [e.g. *McGarr*, 1984; *Campbell*, 1981]. The variation of source properties with tectonic environment or focal depth may affect the shape of the response spectrum as well as the peak ground acceleration. This study uses a simple seismological model of the earthquake source to analyse data from three regions of California to examine how response spectral shapes vary with focal depth, tectonic environment, and earthquake magnitude.

DATA

Data recorded in three different regions has been analysed. The three regions were chosen to represent three different tectonic environments. Earthquakes of the 1992 Southern California sequence are predominantly strike-slip. Earthquakes of the 1983 Coalinga sequence are predominantly thrust although strike-slip and normal faulting also occurred. Earthquakes of the 1980 Mammoth Lakes sequence are predominantly a combination of strike-slip and normal faulting.

The 1992 Southern California earthquake sequence included the M 7.4 Landers, the M 6.5 Big Bear, and the M 6.1 Joshua Tree earthquakes. A total of 9 CSMIP ground response recordings [Darragh et al., 1992; CSMIP staff, 1992] and 5 TERRAscope recordings [*Kanamori et al.*, 1990] of the Landers main shock have been analysed. In addition, 40 earthquakes ranging in magnitude from 4.0 to 6.5 recorded at the Pasadena TERRAscope station and 688

microearthquakes (M 1.5 to 3.6) recorded by digital PASSCAL instruments deployed by the Southern California Earthquake Center have been analysed.

Earthquakes from Coalinga include the M 6.7 Coalinga main shock and its larger aftershocks. The main shock was analysed using recordings from 40 CSMIP ground response stations. In addition, 32 recordings of 5 aftershocks (M 5.0 to 6.0) were analysed from CSMIP stations [*Shakal and McJunkin*, 1983; *Shakal and Ragsdale*, 1983]. Aftershocks were also recorded by the U. S. Geological Survey [*Mueller et al.*, 1984] and the analysis includes 32 recordings of 8 earthquakes (M 4.0 to 5.3) and 106 earthquakes from magnitude 2.5 to 4.0.

The data from the Mammoth Lakes area are recordings from the May-June 1980 earthquake sequence recorded by CSMIP [*Turpin*, 1980] and the U. S. Geological Survey [*Mueller et al.*, 1981; *Spudich et al.*, 1981] . A total of 28 recordings of 11 earthquakes ranging from M 4.0 to 6.2 were studied including four magnitude 6-6.2 earthquakes. In addition, 162 earthquakes ranging from 2.5 to 4.0 in magnitude were included in the analysis from data recorded by the USGS.

DETERMINATION OF EARTHQUAKE STRESS DROP

In order to determine the variation of the response spectrum with tectonic environment and focal depth, the data are analysed using a simple seismological model of the earthquake source. The analysis also includes the effect of attenuation. From this analysis, estimates are made of the earthquake stress drop and source Fourier amplitude spectrum for different focal depths and tectonic environments. Finally, the source Fourier spectra are converted to source response spectra.

In order to determine the earthquake stress drop, the Fourier amplitude spectra of S-waves are analyzed by finding non-linear least squares best fits to the spectra. The Fourier spectra are fit to the logarithm of the functional form [*Boatwright*, 1978]

$$D(f) = \frac{\Omega_0 \exp(-\pi f t^*)}{\left[1 + (f/f_c)^{2\gamma}\right]^{1/2}} \qquad (1)$$

where D(f) is the Fourier displacement amplitude, Ω_0 is the low frequency spectral asymptote, f is the frequency, f_c is the corner frequency, γ is the source spectral falloff, and t* is the integral of the travel time divided by the quality factor of attenuation Q. The parameter γ is taken to be 2.0. The parameter t* determines the attenuation. The best fit for a particular spectrum is the combination of parameters that minimizes the sum of squared residuals. The residual at each value of the Fourier spectrum is the spectrum minus the fit to the spectrum. The best fitting combination of parameters is identically the same whether fitting to the displacement, velocity, or acceleration spectrum. An example of a spectral fit is shown in Figure 1.

Stress drops for S-waves are calculated using the equation [*Brune*, 1970, 1971]

$$\Delta\tau = 7/16\ (2\pi f_c/2.34\beta)^3\ M_0 \qquad (2)$$

where $\Delta\tau$ is the stress drop, β is the shear wave velocity, and M_0 is the seismic moment. The moments for S-waves are determined by

$$M_o = 4\pi \rho\beta^3 r\Omega_o/2R_{\theta\phi} \quad (3)$$

where ρ is the density and r is the hypocentral distance. The value of $R_{\theta\phi}$ is determined by the radiation pattern for which an average value of 0.55 is used [*Boore and Boatwright*, 1984]. The shear wave velocity is taken to be 3.3 km/sec and the density 2.9 g/cm^3.

Table 1 lists the M > 4 events studied in this anlaysis and gives average values for the seismic moment and stress drop.

Table 1. M > 4 earthquakes and source parameters.

Event	Mag.	Depth (km)	# stations	log-avg. moment dyne-cm	log-avg. stress drop bars
1980 Mammoth Lakes:					
5/25 16:33	6.1	10.13	1 CSMIP	$7\ 10^{24}$	220
5/25 16:49	6.0	6.28	2 CSMIP	$2\ 10^{24}$	312
5/25 19:44	6.1	15.26	1 CSMIP	$9\ 10^{24}$	281
5/25 20:35	5.7	0.03	1 CSMIP	$3\ 10^{23}$	177
5/26 18:57	5.7	5.61	1 CSMIP	$5\ 10^{23}$	68
5/27 14:50	6.2	14.73	3 CSMIP	$3\ 10^{24}$	289
5/28 5:16	4.9	5.07	2 USGS	$7\ 10^{22}$	90
5/31 10:11	4.3	5.55	5 USGS	$7\ 10^{21}$	181
6/1 06:47	4.5	7.00	3 USGS	$4\ 10^{22}$	255
6/2 10:22	4.0	6.77	4 USGS	$9\ 10^{21}$	59
6/2 20:34	4.1	7.41	5 USGS	$3\ 10^{21}$	116
1983 Coalinga:					
5/2 23:42	6.7	9.65	40 CSMIP	$1\ 10^{25}$	576
5/9 2:49	5.3	11.75	10 CSMIP + 8 USGS	$3\ 10^{23}$	388
5/9 7:40	5.3	9.5	7 CSMIP	$2\ 10^{23}$	345
7/22 2:39	6.0	9.2	7 CSMIP	$2\ 10^{24}$	188
7/22 3:43	5.0	9.6	2 CSMIP	$1\ 10^{23}$	936
7/25 22:31	5.1	9.5	2 CSMIP	$1\ 10^{24}$	689
5/3 15:41	4.8	7.81	2 USGS	$5\ 10^{22}$	191
5/9 3:26	4.5	12.57	6 USGS	$3\ 10^{22}$	365
5/12 13:41	4.7	10.15	3 USGS	$2\ 10^{22}$	37
5/16 14:21	4.0	8.43	5 USGS	$7\ 10^{21}$	31
5/19 11:05	4.3	12.24	3 USGS	$3\ 10^{21}$	44
5/22 8:39	4.5	9.75	3 USGS	$7\ 10^{21}$	55
5/24 9:02	4.6	9.19	2 USGS	$6\ 10^{22}$	474
1992 Landers:					
6/28 11:57	7.4	9	9 CSMIP + 5 TERRAscope	$5\ 10^{26}$	221
6/29 14:13	5.4	9.88	1 TERRAscope	$7\ 10^{23}$	53
6/29 16:01	5.2	1.86	1 TERRAscope	$5\ 10^{23}$	11
6/30 12:34	4.2	4.57	1 TERRAscope	$9\ 10^{21}$	6.1

Event	Mag.	Depth (km)	# stations	log-avg. moment dyne-cm	log-avg. stress drop bars
6/30 14:38	5.0	0.84	1 TERRAscope	$4\ 10^{23}$	7.4
6/30 20:05	4.1	0.57	1 TERRAscope	$6\ 10^{21}$	3.0
7/01 7:40	5.4	9.00	1 TERRAscope	$1\ 10^{23}$	42
7/2 5:16	4.0	0.72	1 TERRAscope	$6\ 10^{21}$	1.6
7/5 21:18	5.4	0.36	1 TERRAscope	$2\ 10^{24}$	7.6
7/6 12:00	4.5	1.80	1 TERRAscope	$2\ 10^{22}$	3.2
7/7 8:21	4.0	3.24	1 TERRAscope	$6\ 10^{21}$	2.0
7/7 22:09	4.4	2.54	1 TERRAscope	$2\ 10^{22}$	10
7/2 2:23	4.9	6.00	1 TERRAscope	$1\ 10^{23}$	9.4
7/18 0:06	4.0	2.62	1 TERRAscope	$2\ 10^{21}$	1.4
7/20 4:08	4.1	0.41	1 TERRAscope	$1\ 10^{22}$	1.5
7/24 7:23	4.0	8.97	1 TERRAscope	$2\ 10^{21}$	1.4
7/24 18:14	5.0	9.08	1 TERRAscope	$4\ 10^{23}$	1.8
7/25 4:31	4.9	5.85	1 TERRAscope	$1\ 10^{23}$	4.2
8/4 19:06	4.0	0.01	1 TERRAscope	$9\ 10^{21}$	1.7
8/8 15:37	4.4	2.84	1 TERRAscope	$6\ 10^{22}$	2.1
8/11 6:11	4.3	0.75	1 TERRAscope	$6\ 10^{21}$	4.7
8/15 8:24	4.8	0.61	1 TERRAscope	$4\ 10^{22}$	22
1992 Big Bear:					
6/28 15:04	6.5	5.00	1 TERRAscope	$4\ 10^{25}$	378
6/28 15:24	4.8	6.00	1 TERRAscope	$4\ 10^{22}$	19
6/28 17:48	4.4	1.18	1 TERRAscope	$2\ 10^{22}$	3.8
7/1 10:32	4.1	0.35	1 TERRAscope	$3\ 10^{22}$	0.8
7/21 21:10	4.1	1.86	1 TERRAscope	$5\ 10^{21}$	16
8/17 20:41	5.3	11.73	1 TERRAscope	$9\ 10^{22}$	20
8/24 13:51	4.3	1.84	1 TERRAscope	$1\ 10^{22}$	4.4
11/27 16:00	5.3	1.54	1 TERRAscope	$2\ 10^{23}$	91
1992 Joshua Tree:					
4/23 4:50	6.1	12.38	1 TERRAscope	$6\ 10^{25}$	15
4/23 13:35	4.1	1.05	1 TERRAscope	$1\ 10^{22}$	1.0
4/23 18:56	4.4	3.42	1 TERRAscope	$9\ 10^{21}$	9.0
4/26 6:26	4.2	0.62	1 TERRAscope	$4\ 10^{22}$	3.7
4/27 3:11	4.2	0.01	1 TERRAscope	$2\ 10^{22}$	8.4
5/2 12:46	4.2	4.03	1 TERRAscope	$5\ 10^{21}$	9.0
5/4 1:16	4.1	5.97	1 TERRAscope	$8\ 10^{21}$	2.3
5/4 16:19	4.9	12.54	1 TERRAscope	$3\ 10^{23}$	3.3
5/6 2:38	4.7	7.31	1 TERRAscope	$8\ 10^{22}$	10
5/18 15:44	4.9	7.10	1 TERRAscope	$1\ 10^{23}$	15
6/11 00:24	4.3	0.82	1 TERRAscope	$5\ 10^{22}$	1.1

VARIATION OF STRESS DROP WITH DEPTH AND REGION

The variation of microearthquake stress drop with depth is shown in Figure 2 for the three regions. Some of the results for microearthquakes are from a previous anlaysis [Lindley and Archuleta, 1992]. A steady increase of earthquake stress drop with depth might be expected since the stress required for shear failure of rock should increase with the overburden pressure [see e.g. *Sibson*, 1974]. This increase of stress drop with depth is observed for Joshua Tree microearthquakes, but not for Coalinga or Mammoth Lakes microearthquakes. There is a large difference in stress drop between the three regions. Coalinga and Mammoth Lakes stress drops are approximately equal and are about a factor of five to ten larger than Joshua Tree stress drops.

A comparison of average stress drop for Joshua Tree microearthquakes and M >4 earthquakes of the 1992 Southern California earthquake sequence is shown in Figure 3. The Joshua Tree microearthquake stress drops are significantly smaller than the M >4 earthquake stress drops. The M >4 earthquake stress drops are still smaller than the stress drops for Coalinga or Mammoth Lakes (Figure 2). Both calculations show an increase of stress drop with depth. For the larger earthquakes (M>6), we expect that most of the radiated seismic energy will typically come from depths greater than about 5 or 6 km. Thus, the relatively low stress drops of the upper 6 km observed for the 1992 Southern California earthquake sequence would not be expected to alter the shape of the spectra of the potentially damaging earthquakes. It is only for earthquakes of magnitude less than about 5 with shallow focal depths that this low stress drop is likely to be observed.

Comparisons of stress drops for microearthquakes and M >4 earthquakes at Coalinga and Mammoth Lakes are shown in Figures 4 and 5. Again, the M >4 earthquakes have significantly higher stress drops than the microearthquakes. The difference between the stress drops at Coalinga and Mammoth Lakes is not significant. Coalinga and Mammoth Lakes M>4 earthquake stress drops are significantly larger than the M>4 earthquake stress drops of the 1992 Southern California earthquake sequence. This agrees with the results from the microearthquakes. This regional variation in the stress drop will result in significant differences in the response spectrum.

The observed stress drop difference between the three regions does not correspond to the expected variation based on tectonic environment [e.g. *Sibson*, 1974]. Based on tectonic environment, it would be expected that stress drops would be greatest at Coalinga (thrust), second greatest for the 1992 Southern California earthquake sequence (strike-slip), and smallest for Mammoth Lakes (normal/strike-slip). There are many other possible factors that could cause a change in stress drop between regions including earthquake repeat times, pore fluid pressure, rheology, or age of fault zones. The cause(s) for the differences in regional stress drops observed in this study are not readily apparent. Thus, while there are significant variations between the regions, it may be too early to attempt to include those variations in the UBC until a better understanding of the fundamental causes is obtained.

VARIATION OF RESPONSE SPECTRUM WITH REGION AND MAGNITUDE

The source parameters from the spectral fits and the seismological source model in equation (1) allow us to estimate the source Fourier amplitude spectrum. For engineering purposes, the response spectrum is usually more important than the Fourier spectrum. In order to calculate the response spectrum from the Fourier spectrum, random-vibration theory is used following *Joyner and Boore* [1988].

In order to compare the source response spectra between the three regions, hypothetical Fourier amplitude spectra are determined for a M6-6.5 event in each region (Figure 6). For the 1992 Southern California earthquake sequence, source parameters from the M 6.1 Joshua Tree and

M 6.5 Big Bear earthquakes were averaged together. For Coalinga, source parameters from the M 6.7 main shock and the M 6.0 aftershock were used, and for Mammoth Lakes, source parameters from the four main shocks (M 6.0 to 6.2) were averaged. The source response spectra were then calculated from the Fourier spectra following *Joyner and Boore* [1988].

As expected, the results indicate that the source response spectra at Coalinga and Mammoth Lakes are similar while the response spectra for the Southern California earthquake sequence are significantly different (Figure 7). The amplitude of the source response spectrum for the hypothesized M6-6.5 Southern California earthquake is larger at long periods and smaller at short periods compared to Coalinga or Mammoth Lakes. The reason for this is that the seismic moment is larger and the stress drop smaller for the same magnitude earthquake for the Southern California earthquake sequence as compared to Coalinga or Mammoth Lakes. The seismic moment controls the response at long periods boosting these levels and causing the source response spectrum for the Southern California earthquake to be larger at long periods.

It is interesting to compare one of the source response spectra (in this case Coalinga) to the 1991 UBC normalized response spectra (Figure 8). Also included is the source response spectrum with attenuation added ($t^* = 0.05$ s). The source response spectrum without attenuation is much larger than the UBC spectra at short periods. However, the shape of the source response spectrum with attenuation matches the shape of the UBC spectra, at least qualitatively. Thus, the rolloff of the response spectra typically observed for short periods appears to be controlled by attenuation while the falling amplitudes at long periods is controlled by the earthquake source.

It is also interesting to compare the source response spectra for different magnitude earthquakes of the 1992 Southern California earthquake sequence to see if magnitude affects the shape of the response spectra (Figure 9). From Figure 9 it appears that when the difference in magnitude is greater than or approximately 2, the response spectral shapes begin to become significantly different. The larger magnitude earthquake is observed to have greater amplitudes at long periods compared to the smaller magnitude earthquake. The explanation for this change in the source response spectral shape is that the corner frequency (see equation (1) and Figure 1) is smaller for the larger magnitude earthquake. This smaller corner frequency causes a boost in the source response spectrum for the larger earthquake at longer periods.

REFERENCES

Boatwright, J. (1978). Detailed spectral analysis of two small New York State earthquakes, *Bull. Seism. Soc. Am.*, **68**, 1117-1131.

Boore, D. M. and J. Boatwright (1984). Average body-wave radiation coefficients, *Bull. Seism. Soc. Am.*, **74**, 1615-1621.

Brune, J. N. (1970). Tectonic stress and the spectra of seismic shear waves from earthquakes, *J. Geophys. Res.*, **75**, 4997-5009. (Correction *J. Geophys. Res.*, **76**, 5002, 1971.)

Campbell, W. C. (1981). Near-source attenuation of peak horizontal acceleration, *Bull. Seism. Soc. Am.*, **71**, 2039-2070.

CSMIP staff (1992). Preliminary processed strong-motion data for the Landers earthquake of 28 June 1992, *California Division of Mines and Geology Report OSMS 92-11.*

Darragh, R., T. Cao, C. Cramer, F. Su, M. Huang, and A. Shakal (1992). Processed CSMIP strong-motion records from the Landers, CA earthquake of 28 June 1992: Release No. 2, *California Division of Mines and Geology Report OSMS 92-13.*

Joyner, W. B. and D. M. Boore (1988). Measurement, characterization, and prediction of strong ground motion, in *Earthquake Engineering and Soil Dynamics II - Recent Advances in Ground-Motion Evaluation*, J. L. Von Thun, editor, American Society of Civil Engineers Geotechnical Special Publication No. 20, 43-103.

Kanamori, H., E. Hauksson, and T. Heaton (1990). TERRAscope and CUBE project at Caltech, *Eos*, **72**, 564.

Lindley, G. T. and R. J. Archuleta (1992). Earthquake source parameters and the frequency dependence of attenuation at Coalinga, Mammoth Lakes, and the Santa Cruz Mountains, California, *J. Geophys. Res.*, **97**, 14,137-14,154.

McGarr, A. (1984). Scaling of ground motion parameters, state of stress, and focal depth, *J. Geophys. Res.*, **89**, 6969-6979.

Mueller, C., P. Spudich, E. Cranswick, R. Archuleta (1981). Preliminary analysis of digital seismograms from the Mammoth Lakes, California earthquake sequence of May-June, 1980, U.S. Geological Survey Open-File Report 81-155.

Mueller, C. S., E. Sembera, and L. Wennerberg (1984). Digital recordings of aftershocks of the May, 2 1983 Coalinga, California earthquake, U.S. Geological Survey Open-File Report 84-697.

Shakal, A. F. and R. D. McJunkin (1983). Preliminary summary of CDMG strong-motion records from the 2 May 1983 Coalinga, California, earthquake, California Division of Mines and Geology Report 83-5.2 (rev. 3).

Shakal, A. F. and J. T., Ragsdale (1983). Strong motion data from the Coalinga, California earthquake and aftershocks, in *The 1983 Coalinga, California, Earthquakes*, J. H. Bennett and R. W. Sherburne, editors, *Calif. Div. Mines Geol. Spec. Publ. 66*, 113-126.

Sibson, R. (1974). Frictional constraints on thrust, wrench, and normal faults, *Nature*, **249**, 542-544.

Spudich, P., E. Cranswick, J. Fletcher, E. Harp, C. Mueller, R. Navarro, J. Sarmiento, J. Vinton, R. Warrick (1981). Acquisition of digital seismograms during the Mammoth Lakes, California, earthquake sequence May-June 1980, U.S. Geological Survey Open-File Report 81-38.

Turpin, C. D. (1980). Strong-motion instrumentation program results from the May, 1980, Mammoth Lakes, Califorina earthquake sequence, in *Mammoth Lakes, California earthquakes of May 1980*, R. W. Sherburne, editor, *Calif. Div. Mines Geol. Spec. Publ. 150*, 75-90.

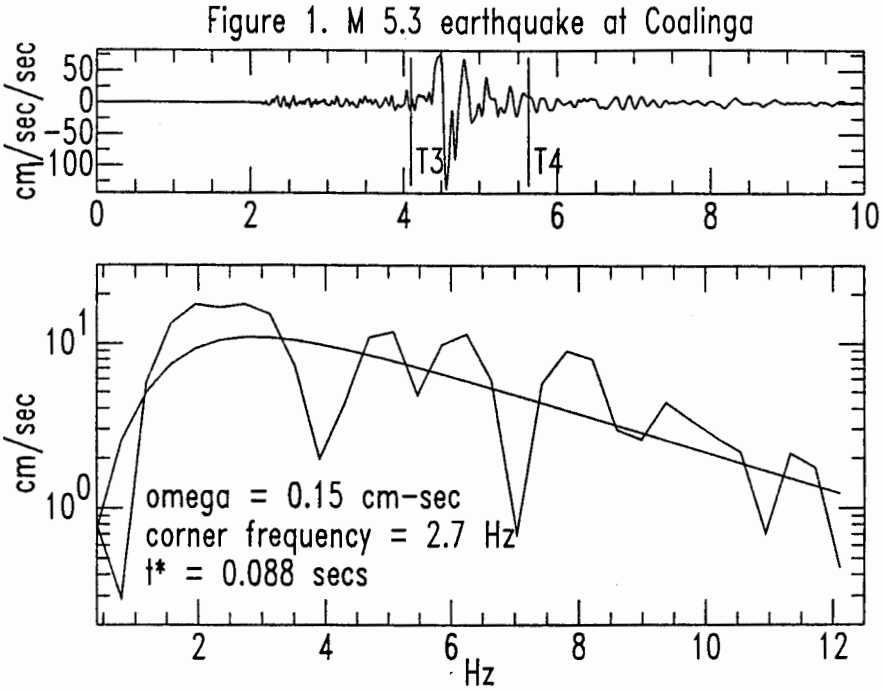

Figure 1. Example determination of earthquake source parameters and attenuation from the Fourier amplitude spectrum (M 5.3 aftershock from Coalinga). T3 and T4 mark the window for which the Fourier amplitude spectrum was calculated. The smooth curve in the spectrum is the fit to the Fourier spectrum.

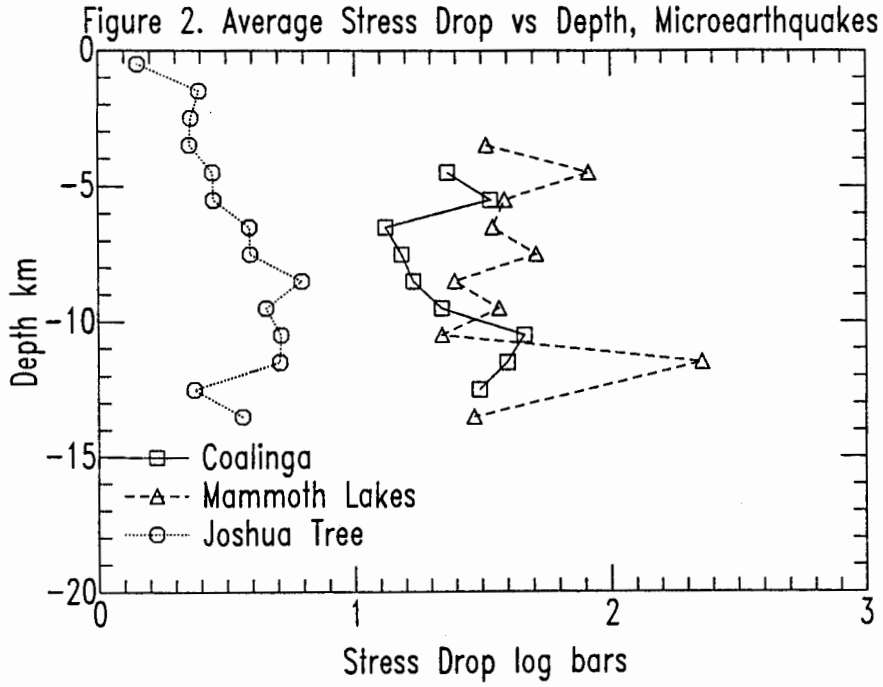

Figure 2. Variation of earthquake stress drop with depth for microearthquakes from three different regions of California. Data points are log-average stress drops for large numbers of microearthquakes in the three regions.

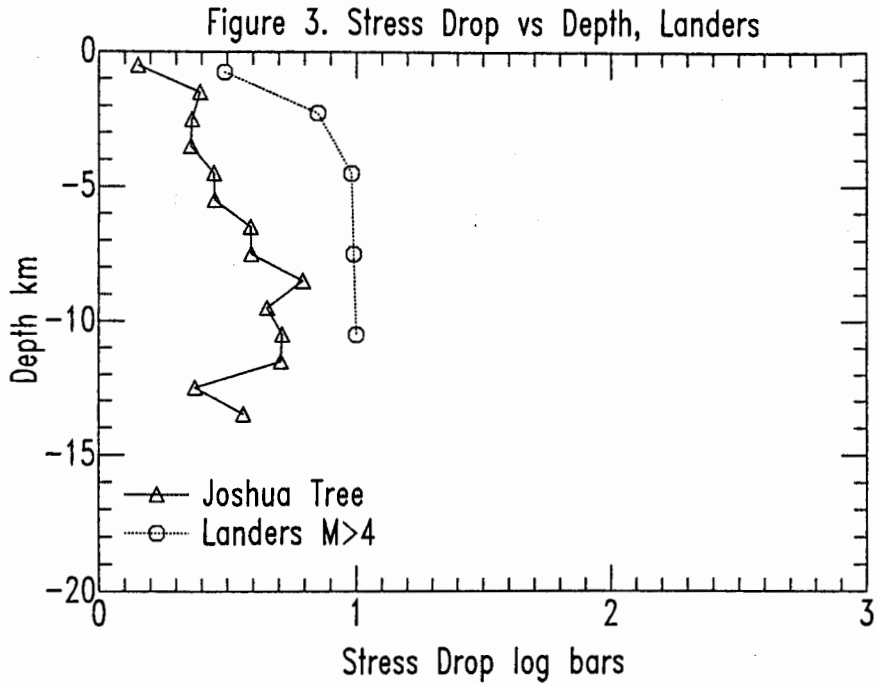

Figure 3. Stress drop versus depth for microearthquakes and M > 4 earthquakes from the 1992 Southern California earthquake sequence. Data points are log-average stress drops for the different depths.

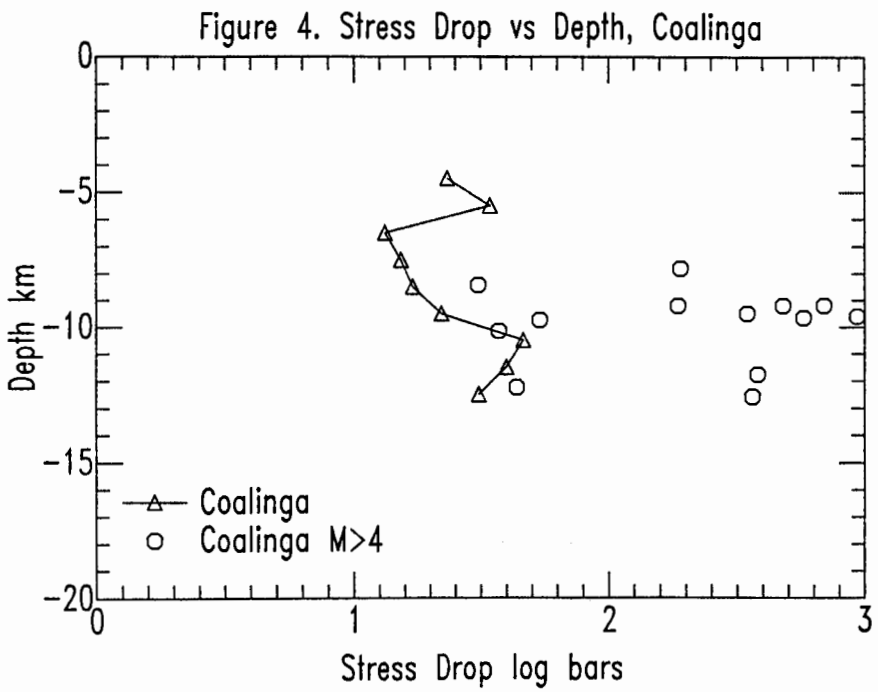

Figure 4. Stress drop versus depth for microearthquakes and M > 4 earthquakes from Coalinga. Circles are for individual M > 4 earthquakes.

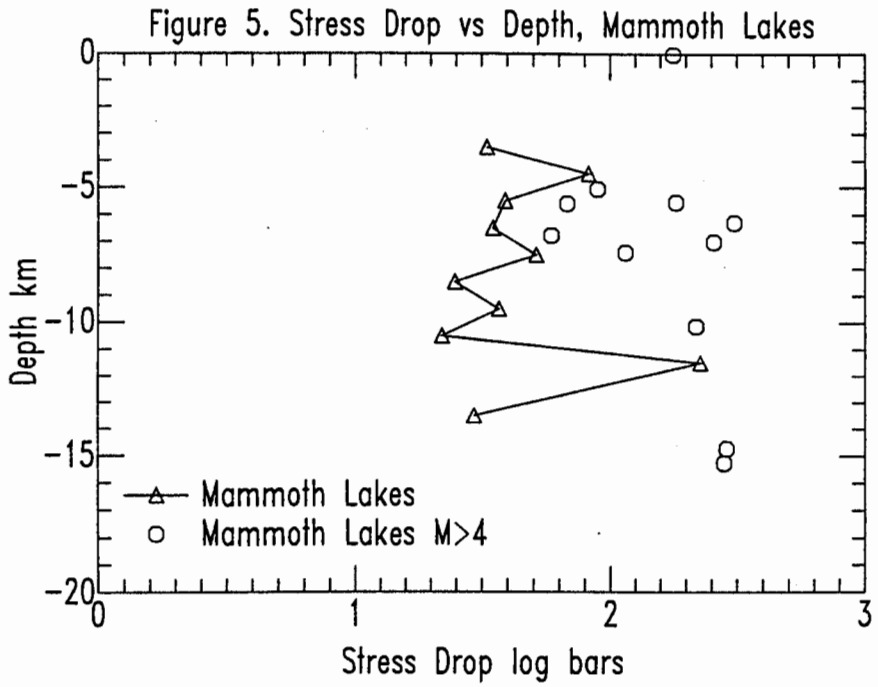

Figure 5. Stress drop versus depth for microearthquakes and M > 4 earthquakes from Mammoth Lakes. Circles are for individual M > 4 earthquakes.

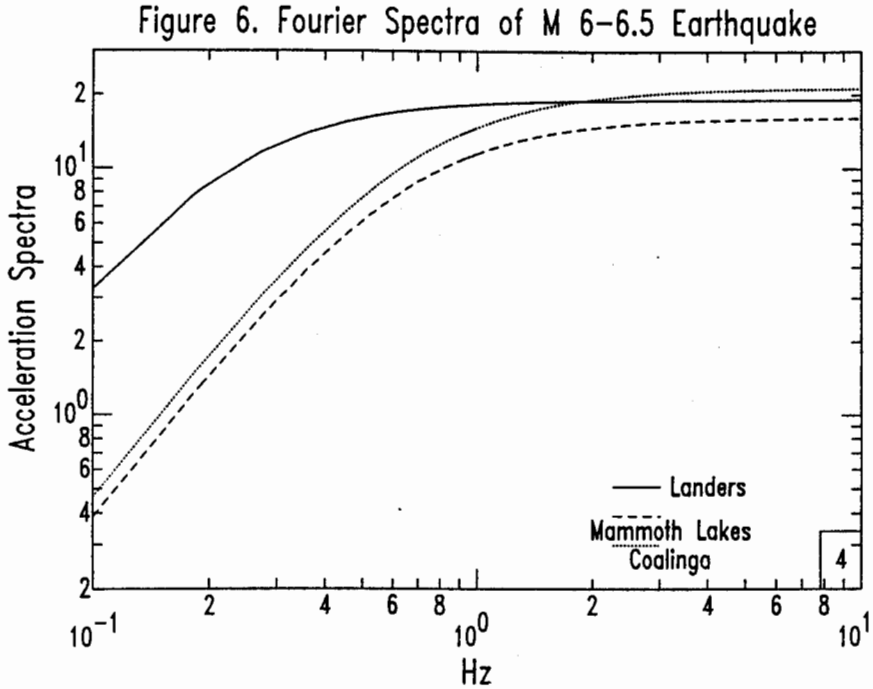

Figure 6. Source Fourier amplitude spectra for the three different regions for an hypothetical M 6-6.5 earthquake. The scale of the amplitude spectrum is arbitrary and depends on distance from the source.

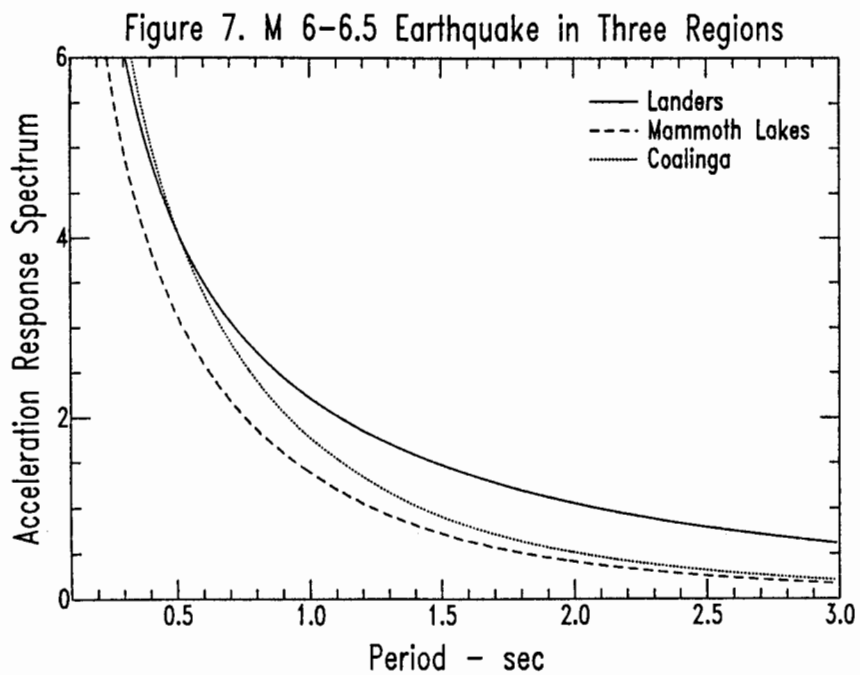

Figure 7. Source response spectra for the three different regions for an hypothetical M 6-6.5 earthquake. The scale of the amplitude spectrum is arbitrary and depends on distance from the source.

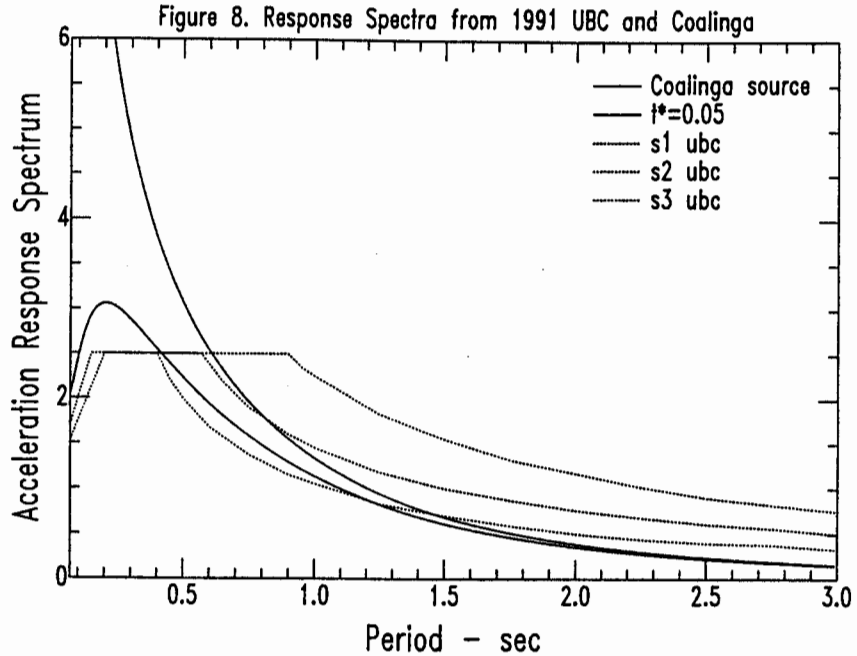

Figure 8. Source response spectrum for the Coalinga M 6-6.5 hypothetical earthquake, response spectrum with attenuation (t*=0.05 s), and normalized response spectra from the 1991 Uniform Building Code.

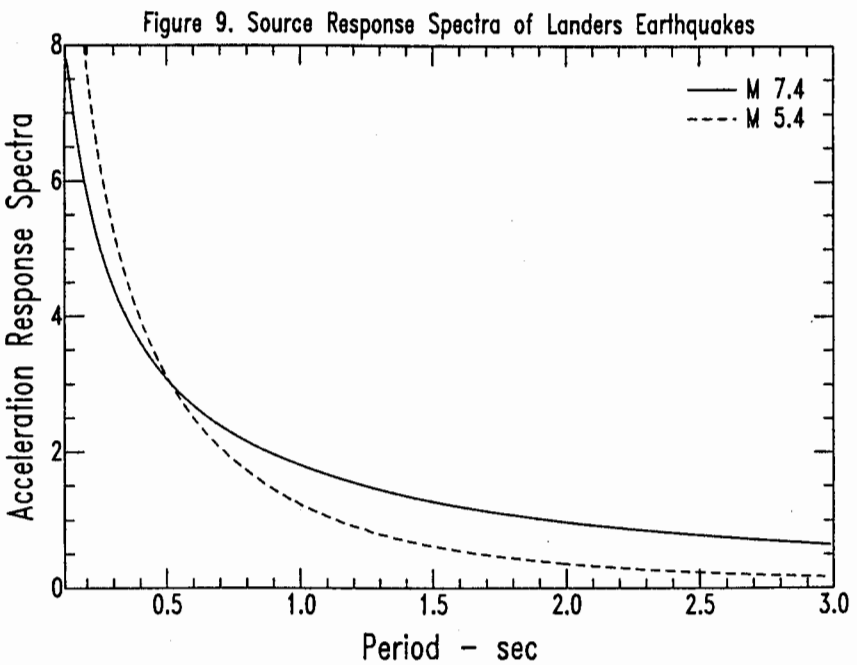

Figure 9. Source response spectra for the M 7.4 Landers main shock and for a nearby M 5.4 aftershock.